 https://doi.org/10.3311/PPci.21641

Periodica Polytechnica Civil Engineering, 67(3), pp. 914–924, 2023

Role of Nonlinearity in the Soil in Earthquake-Resistant Design of Structures

Yaseen Shayah[1*], László P. Kollár[1]

[1] Department of Structural Engineering, Faculty of Civil Engineering, Budapest University of Technology and Economics, 1111 Budapest, Műegyetem rkp. 3, Hungary
[*] Corresponding author, e-mail: yaseen.shayah@epito.bme.hu

Received: 04 December 2022, Accepted: 07 May 2023, Published online: 17 May 2023

Abstract

The nonlinearity of the soil may considerably affect the response of structures subjected to seismic events. This paper aims to show under which circumstances geometry, soil, and earthquake-type; the nonlinearity is important. A simple model based on a 1D shear column was developed to calculate the maximum shear strain (γ) in the soil subjected to earthquake excitation. It was found that γ is a function of peak ground acceleration PGA and the maximum horizontal ground displacement (Δ). EC8 provides an expression for calculating Δ that is independent of the soil thickness. It was found that this expression is conservative for shallow layers and underestimates γ for thick ones, as a result, improvements have been suggested. By performing several time history analyses, simple formulas are developed which enable the designer to assess when nonlinearity must be taken into account. Four curves based on soil thickness and peak ground acceleration have been introduced for different soil types (A, B, C, and D) using a limit value of $\gamma = 10^{-4}$. These curves show that depending on the soil depth, the threshold acceleration of nonlinear soil behavior is around 0.48, 0.36, 0.29, and 0.10 m/s^2 for soil types A, B, C, and D, respectively. Obviously, nonlinear analysis must be performed for shallow soil layers under moderate seismicity.

Keywords

soil-structure interaction, SSI, seismic analysis, shear strain, linear, nonlinear

1 Introduction

Structures are often analyzed assuming a rigid (built-in) connection to the ground. When structures are subjected to earthquakes, this assumption may lead to unacceptably inaccurate results, and the soil-structure interaction (SSI) must be taken into account [1, 2].

Soil-structure interaction can be considered in two ways: direct method and substructure approach. These approaches are well documented in Wolf's textbook [3]. In the direct method, the soil and the structure are included within the same model and analyzed in a single step as a complete system; it is applicable to both linear and nonlinear analyses [4]. In the substructure approach, the structure's response is obtained by superposition; hence this method has only been applied to linear systems [4, 5]. Several studies have examined the impact of soil-structure interaction on various systems, including single-degree-of-freedom systems with liquid dampers, outrigger-braced buildings with belt truss systems, braced buildings with Buckling-restrained braces, and seismic response of soil-structure systems using wavelet transform methodology [6–9].

The soil stress-strain relationships are not always linear, particularly when the shear strain is expected to be high enough to produce a nonlinear hysteresis loop in the cyclic stress-strain relationship [10, 11]. Shear stress τ and shear strain γ are linked by the shear modulus G:

$$\tau = G(\gamma)\gamma \ . \tag{1}$$

The shear modulus of the soil varies with the amplitude of the cyclic shear strain. The shear modulus is high and uniform at low strain amplitudes but decreases as the strain amplitude increases. The shear modulus of soil decays nonlinearly as the strain amplitude increases [1], as shown in Fig. 1 [12].

Based on laboratory tests Vucetic [10] has divided the change of soil stiffness and strain into three regions: very small strain, small strain, and large strain, respectively, as shown in Fig. 1. He defined two shear-strain thresholds related to soil nonlinearity: linear cyclic γ_{tl}, which called nonlinearity threshold by Ishihara; and volumetric shear strains γ_{tv} [5]. There is a general understanding

Cite this article as: Shayah Y., Kollár, L. P. "Role of Nonlinearity in the Soil in Earthquake-Resistant Design of Structures", Periodica Polytechnica Civil Engineering, 67(3), pp. 914–924, 2023. https://doi.org/10.3311/PPci.21641

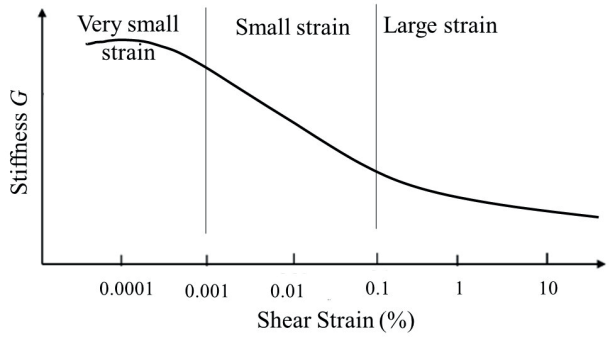

Fig. 1 Stiffness-strain behavior of soil with typical strain ranges [12]

that nonlinearity in the soil depends primarily on the shear strain [1]. Although nonlinearity occurs already around $\gamma \approx 10^{-5}$ in engineering analysis, a quasi-linear calculation may be performed when the shear strains do not exceed $\gamma \approx 10^{-4}$ [13, 14].

Note, however, that somewhat lower value $\gamma \approx 10^{-4}$ should be used for sand while higher value $\gamma \approx 10^{-3}$ for clay [15].

A few researchers claim that even for moderate seismicity ($a_g \approx 0.1$ g ≈ 1 m/s^2) nonlinearity cannot be neglected [16, 17]. Wu et al. [18] determined peak ground acceleration (PGA) thresholds for 6 locations from 0.20 to 0.80 m/s^2 using seismic records from KiK-net in Japan. In Parkfield, California, Rubinstein [19] discovered that at low levels of shaking (around 0.35 m/s^2) nonlinear site response could occur. Ghofrani et al. [20] estimated PGA nonlinearity thresholds for 49 sites from 0.04 to 1.50 m/s^2 using seismic records from KiK-net in Japan. Wang et al. [21], using acceleration time histories data at eight KiK, determined that the stiffness and plasticity index are primarily responsible for the threshold acceleration of nonlinear soil behavior, which ranges from 0.2 to 1 m/s^2. There is no comprehensive investigation of the size of earthquakes (scale or peak ground acceleration PGA) when nonlinearity in soil (material nonlinearity) must be taken into account. As a consequence, we wish to develop a model that can predict the response of soil by utilizing a few parameters, including the magnitude of an earthquake and the properties of the ground (depth and type of soil). These specific parameters are provided in EC8.

2 Problem statement

Our aim is to develop a simple model and a design procedure with the aid of which the designer can decide whether nonlinearity plays a role in the SSI. It is assumed that the earthquake is characterized by the response spectrum (given, e.g., in EC8) displacement (Δ; an option is the value given by the expression in EC8, [22]), while the soil geometry is given by the depth above the bedrock (h).

Based on the developed procedure, we wish to investigate the question whether nonlinearity is important or not under moderate seismicity.

3 Assumptions and basic hypothesis

To understand the response of the soil subjected to earthquakes, a finite depth layer on the rock with infinite horizontal dimensions is considered (Fig. 2(a)). Although it is a 3D problem, for horizontal excitation, it is sufficient to consider a 1D shear column (Fig. 2(b)), where S waves develop.

In the analysis, the soil is given by G and ν, while $\xi = 5\%$ damping ratio is considered.

For simple modeling, it is assumed that a sinusoidal wave develops in the soil Fig. 3. The accuracy of this assumption will be investigated in Section 5. The displacement is given by:

$$u = \Delta \cos\left(\frac{2\pi z}{L}\right), \tag{2}$$

where Δ is the amplitude of the wave, while L is the wavelength. The angular strain is calculated by:

$$\gamma = \frac{\partial u}{\partial z} + \frac{\partial w}{\partial x}, \tag{3}$$

which, since $\partial w/\partial x \approx 0$, results in

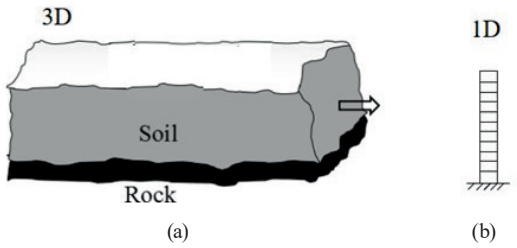

Fig. 2 Simplified model of a soil layer; (a) 3D model, (b) 1D shear column

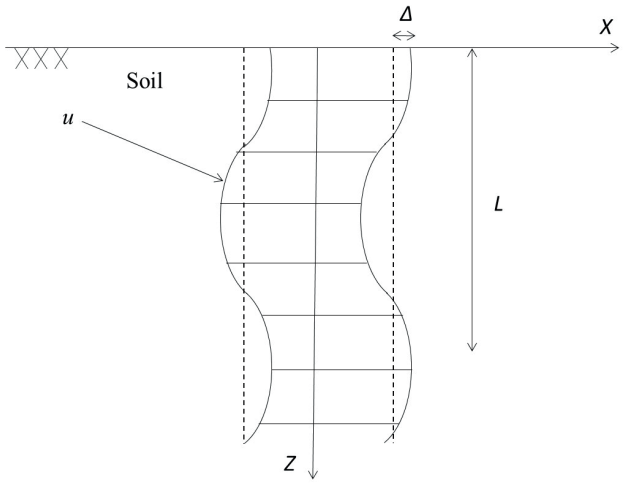

Fig. 3 Typical deformed shape of a column of the soil in the simplified analysis

$$\gamma = \frac{\partial u}{\partial z} = -\frac{2\pi}{L}\Delta \sin\left(\frac{2\pi z}{L}\right). \tag{4}$$

The maximum shear is calculated by replacing the $\sin(2\pi z/L)$ function with unity; thus, we have

$$\gamma = -\frac{2\pi}{L}\Delta. \tag{5}$$

The wavelength L is approximated by the following reasoning. For shallow layers, a quarter-wave is assumed in the soil [23], Fig. 4(a).

$$L = 4h \tag{6}$$

For a deep layer, full waves may develop in the soil, and for trigonometric excitation with a period of vibration T, the wavelength is:

$$L = Tv = v / f, \tag{7}$$

where v is the shear wave velocity, and $f = 1/T$ is the excitation frequency. (The value of T for real earthquakes will be discussed later).

For an intermediate thickness of the soil, it was expected that an interpolation must be performed (see dashed line in Fig. 5), but as it will be discussed in Section 5.1, it is unnecessary.

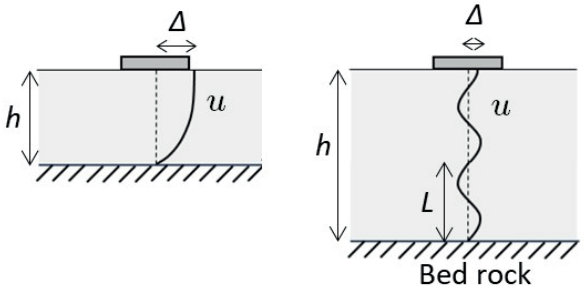

(a) (b)

Fig. 4 Deformation of the soil for shallow (a) and deep (b) layers

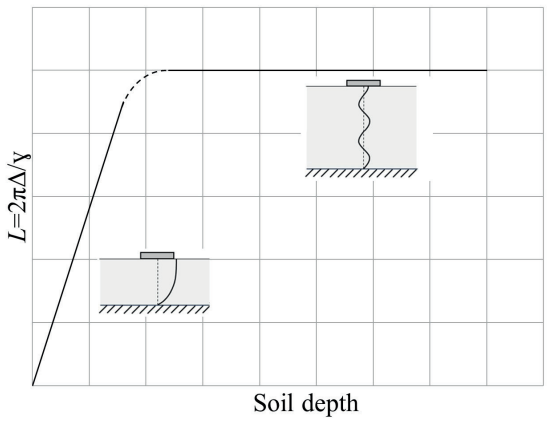

Fig. 5 Expected soil depth versus wavelength curve

The shear wave velocity (v) is related to the shear modulus as [24]:

$$G = pv^2, \tag{8}$$

where ρ is the density. The maximum total horizontal displacement $\bar{\Delta}$ is given in EC8 by:

$$\bar{\Delta} = d_g = 0.025 a_g S T_C T_D, \tag{9}$$

where a_g is the design ground acceleration on type A ground. The values of the periods T_C, T_D and S - soil factor - describe the

shape of the elastic response spectrum, which depends on the ground type, see Fig. 6.

Note that $\bar{\Delta}$ is the total displacement, while Δ is the

relative displacement between the ground and the bedrock. $\bar{\Delta}$ can be used as an upper limit for Δ, i.e., it is a conservative approximation.

Since an approximation is given for L by Eq. (6) and Eq. (7), γ can be directly calculated by Eq. (5).

Now it must be investigated whether this simple model is reasonable or not.

4 Approach

4.1 Model description

The 1D shear column was considered in ANSYS Mechanical APDL 2020 by applying constraints on the vertical displacement. In the analysis, G was defined, the Poisson's ratio $v = 0.3$, and the height of the column and the excitation were varied.

Two kinds of excitations of the bedrock were investigated:

- Harmonic excitation ($a_g = \Delta \sin\frac{2\pi}{T}t$) where T was varied; and
- Earthquake excitations (both artificial and real records).

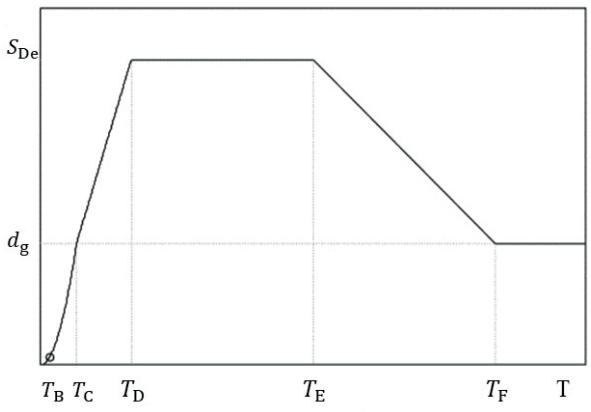

Fig. 6 Elastic displacement response spectrum [22]

4.2 Finite Element Model

The finite element models are built in ANSYS 2020R1 Mechanical APDL software, and transient analysis is performed. The stripe width is 1.5 m with different soil depths, Fig. 7. The soil is modeled with the linear and Classic Drucker-Prager material models for the nonlinear analysis. Plane183 element has been used in the modeling, which is a higher-order 2-D element with 8 or 6 nodes. This element has two degrees of freedom at each node: displacement in the x and y directions [25]. The properties of all soil types analyzed are summarized in the table of Section 5.2.

Vertical constraints have been applied on the vertical sides and at the bottom (bedrock). The earthquake is modeled by applying a given acceleration in the x direction at the boundary, Fig. 7. The mesh size used in all models is 0.25 m. The sensitivity analysis of the mesh size will be shown in the next section.

4.3 Mesh sensitivity analysis

Kuhlemeyer and Lysmer [26] recommend that mesh size should be less than one-eight of the wavelength associated with the maximum frequency component f_{max} of the input wave. This suggestion is commonly used in dynamic modeling to obtain reliable results. The required mesh size is:

$$\frac{L}{8} = \frac{Tv}{8} = \frac{v}{8f_{max}}. \tag{10}$$

The frequency content of typical earthquakes is in the range of 0.45 Hz and 2.82 Hz [27], this range was obtained by analyzing the 44 far-field records of FEMA [28]. By substitution, the lowest velocity, 100 m/s, and $f = 2.82$ Hz, give the average element size of 4.43 m. The mesh size used in all models is 0.25 m, which is much less than 4.43 m.

The converged solution is analyzed to determine how much it varies with each mesh after the same simulation is performed with grids of varying resolutions. Soil type C (v_s = 250 m/s) with the soil depth, 50 m and 200 m, and four different mesh sizes have been applied (0.25, 0.3 0.5 and 1.5 m). Table 1 shows mesh sensitivity analysis results, and Fig. 8 presents the variations of the relative displacement at top along different mesh size for the model 1.5 m width and 50 m depth. It is clear when increasing the mesh size to 1.5 m a different response has been got.

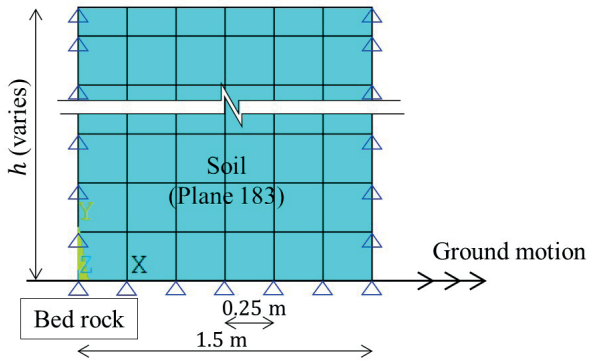

Fig. 7 Finite element model (generated mesh and boundary conditions)

5 Results and discussion

Our hypothesis given in Section 3 is investigated below. Both harmonic and earthquake excitations are considered. The results obtained from the analyses are summarized in the following two subsections.

5.1 Harmonic excitation

To obtain the steady-state solution of the displacements, harmonic analysis is performed for three different types of soils (A, B, and C) at three different excitation frequencies ($T = 1/f$=0.6, 1.2, and 2.4s, which is in the range of the frequency content of typical earthquake records. The results, as shown in Fig. 9 and Fig. 10, agree well with Eq. (6) (inclined line) and Eq. (7) (horizontal line), and surprisingly no intermediate solution is needed (shown by the dashed line in Fig. 5).

Table 1 Mesh sensitivity analysis results

Model	Mesh [m]	Disp [m]	Strain	Diff %
50 × 1.5 m	0.25	9.296E-02	2.7880E-03	-
	0.30	9.296E-02	2.7880E-03	0.000%
	0.50	9.296E-02	2.7880E-03	0.002%
	1.50	1.050E-01	2.8772E-03	3.201%
200 × 1.5 m	0.25	2.624E-01	1.8810E-03	-
	0.30	2.624E-01	1.8816E-03	0.030%
	0.50	2.624E-01	1.8786E-03	-0.161%
	1.50	2.939E-01	1.9124E-03	1.768%

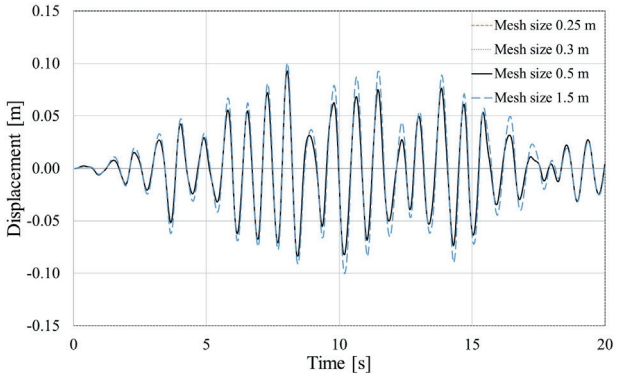

Fig. 8 Relative displacement variations for model 50 × 1.5 m with different mesh sizes

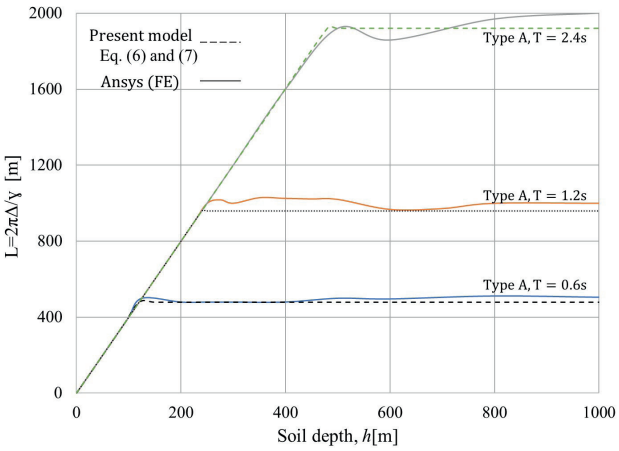

Fig. 9 Soil depth versus wavelength for harmonic excitation (Soil type A, v = 800 m/s and three different frequencies)

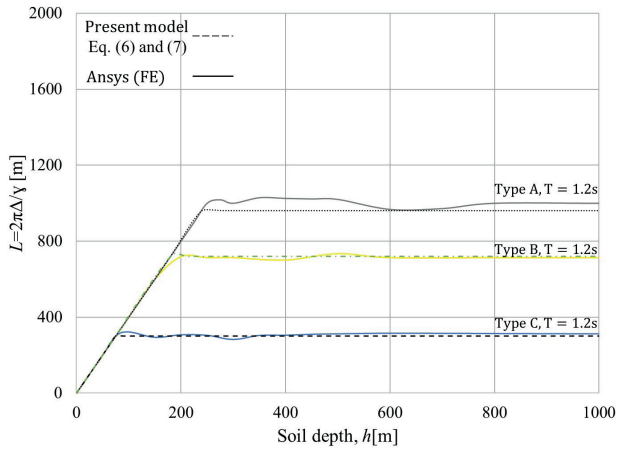

Fig. 10 Soil depth versus wavelength for harmonic excitation (Soil type A v = 800 m/s, B v = 600 m/s, and C v = 250 m/s)

The soil depth, which separates the shallow and deep layers, can be calculated from the intersection of Eqs. (6) and (7).

5.2 Earthquake – artificial records

Artificial earthquake records were generated for four soil types given by EC8 (see Table 2). For each response spectrum, 12 independent records were generated.

The peak ground accelerations (a_g) can take an arbitrary value. For simplicity, only 4 out of the 12 responses for type A is given in Fig. 11 and in Appendix A (Fig. 27 to Fig. 29) for soil types B, C, and D, respectively. It is worth noting that EC8 provides different ground profiles based on parameters including velocity, which are selected to represent a wide range of ground types. The length of acceleration records is 20 s.

Altogether, more than 1000 time history analyses were performed. The results are shown in Fig. 12 to Fig. 15. The soil depth varied between 25 and 2000 m.

Table 2 Properties of the analyzed soil types

Soil Type	v [m/s]	ρ [kg/m^3]	G_{max} [N/m^2]	ξ
A	800	1800	1.15E+09	0.05
B	600	1800	6.48E+08	0.05
C	250	1800	1.13E+08	0.05
D	100	1800	1.80E+07	0.05

v_s shear wave velocity, ρ density, G_{max} shear modulus, ξ damping ratio

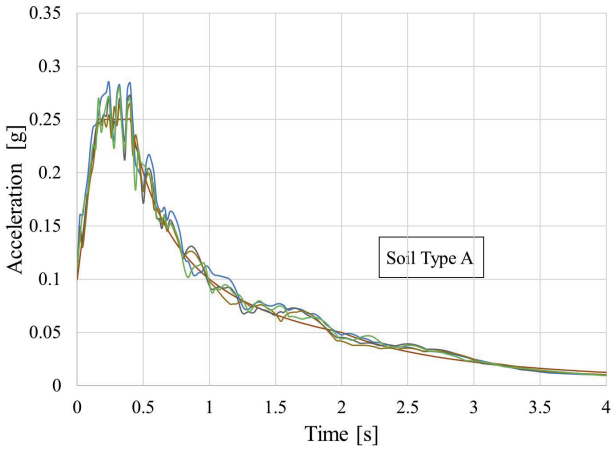

Fig. 11 Response spectra of artificial earthquake records generated for the given response spectrum to EC8 (a); Type A

First, the peak ɣ-s and the corresponding peak Δ-s were determined. $2\pi\Delta/\gamma$ (which is equal to a replacement wavelength L) is shown as a function of the soil depth.

The beginning of the curves agrees well with Eq. (6), which means that clearly, a quarter-wave develops (Fig. 5).

Recall that for a cyclic excitation, there is a clearly visible plateau (Figs. 9 and 10), which is determined by the period of vibration, T. This is not the case for earthquake records due to the different frequency content of the records.

Note, however, that a clear lower bound (conservative) approximation can be given by limiting the soil depth by h_L = 650 m. We may calculate L as follows:

$$L = \min\begin{Bmatrix} 4h \\ 4h_L \end{Bmatrix}. \tag{11}$$

The graphs (Fig. 12 to Fig. 15) show excellent agreement at the beginning but slightly scattered curves at a specific soil depth, which varies slightly between soil types. Because the goal was to create a simple model for estimating soil nonlinearity, a conservative lower-bound approximation that may occasionally overestimate was chosen.

6 Importance of nonlinearity as a function of PGA

As it was shown above, the angular strain in the soil can be approximated by Eq. (5).

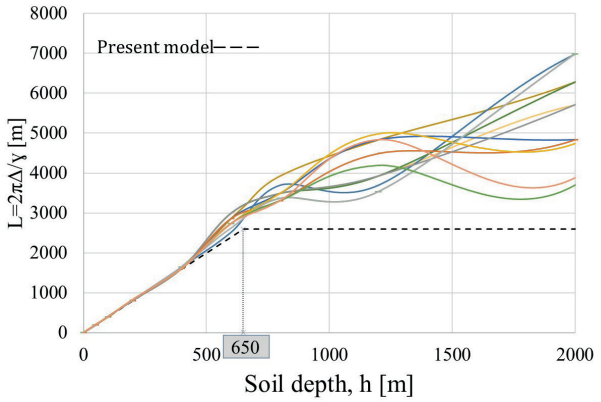

Fig. 12 Results due to artificial earthquake records, Type A (v = 800 m/s)

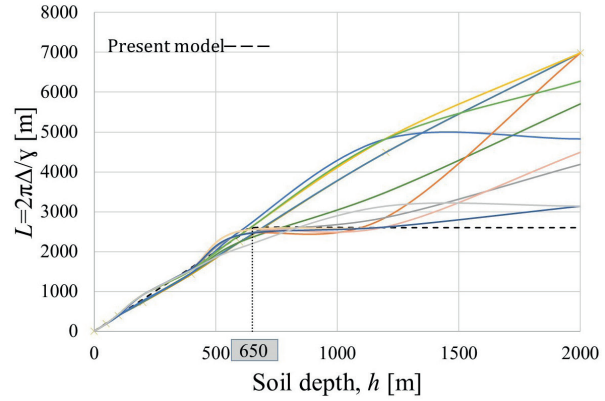

Fig. 13 Results due to artificial earthquake records, Type B (v = 600 m/s)

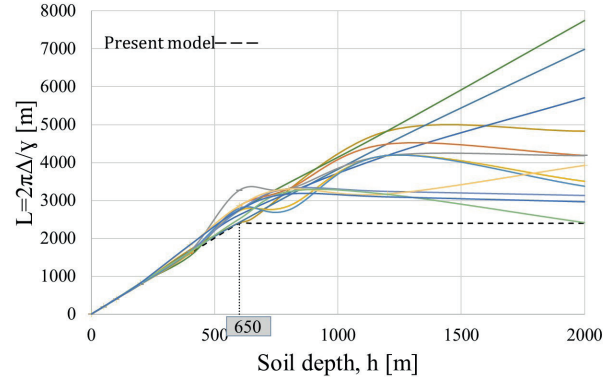

Fig. 14 Results due to artificial earthquake records, Type C (v = 250 m/s)

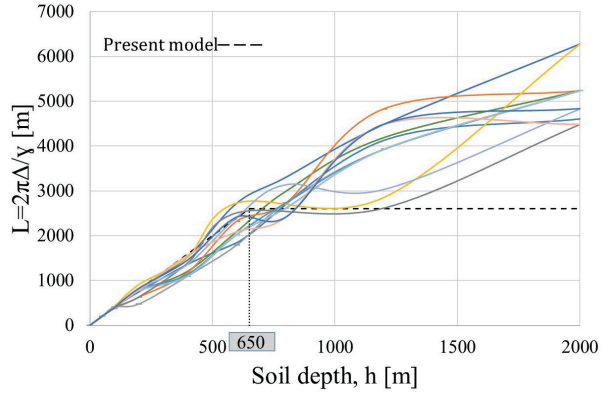

Fig. 15 Results due to artificial earthquake records Type D (v = 100 m/s)

L is approximated by Eqs. (6) and (7). While Δ can be approximated by Eq. (9). $\bar{\Delta}$ is proportional to PGA; we write

$$\bar{\Delta} = a_g \Delta_0 \,, \tag{12}$$

where Δ_0 is the maximum soil displacement for unit PGA, which according to EC8.

$$\Delta_0 = 0.025 S T_C T_D \tag{13}$$

Eq. (5) and Eq. (12) result in

$$a_g = L\alpha \,, \tag{14}$$

where,

$$\alpha = \frac{\gamma}{\Delta_0}\frac{1}{2\pi} \,. \tag{15}$$

For an engineering analysis, nonlinearity can be neglected when $\gamma \le \gamma_L \approx 10^{-4}$. By introducing this value in Eq. (15), we obtain:

$$\alpha_0 = \frac{10^{-4}}{\Delta_0}\frac{1}{2\pi} \,. \tag{16}$$

Using this expression, together with Eq. (14) we have:

$$a_g = L\frac{10^{-4}}{\Delta_0}\frac{1}{2\pi} \,, \tag{17}$$

which is shown for soil type A (v = 800 m/s) in Fig. 16.

The curve shown in Fig. 16 is based on γ_L/Δ_0, using the approximate Δ_0 value of EC8 (Eq. (9)). However, it was found numerically that Eq. (9) may seriously underestimate both the absolute and relative displacement. To obtain a reliable solution, in the following section, we will present a simple refinement of the calculation of Δ_0.

Note that these results are based on a limited number of earthquake records and the results are scattered; hence a general application of these expressions is not recommended.

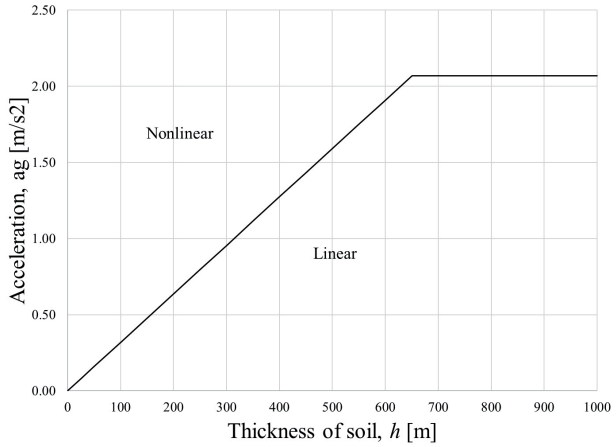

Fig. 16 Linear domain (below the solid line), Soil type A (v = 800 m/s), according to Eqs. (11), (13) and (17)

6.1 Enhancement of soil displacement Δ_0

Based on the calculations using the aforementioned artificial earthquake records (Δ/a_g) versus soil depth (h) are presented for four different soil types to show the variation of Δ_0 along soil depth. An illustration of one of these curves - soil type A - is shown in Fig. 17.

Fig. 17 shows that for shallow soil layers (below around 100 m), EC8 overestimates Δ_0, while for higher values Δ_0 is underestimated. A reasonable envelope can be drawn by two straight lines, as illustrated in Fig. 17. The corresponding expressions are given in the first row of Table 3. Using similar reasoning, expressions were suggested for soil types B, C, and D, which are also given in the same table.

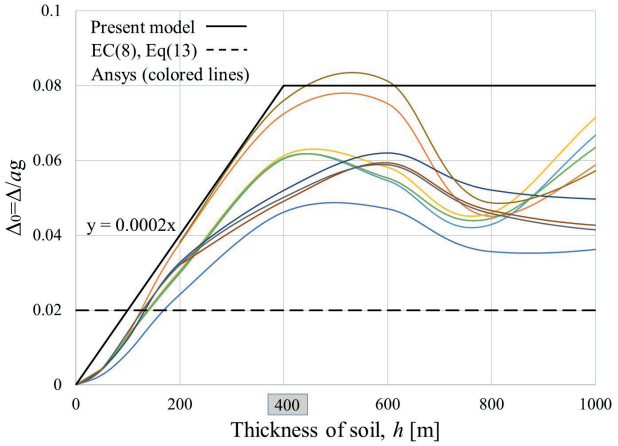

Fig. 17 Δ/a_g versus soil depth due to artificial earthquakes - Type A (v = 800 m/s)

Table 3 Proposed models to calculate the soil displacement ($h \leq 1000$ m)

Soil Type	Soil depth	
	$h \leq 400$ m	$h > 400$ m
A	$\frac{\Delta}{a_g} = \max\left\{\begin{array}{l} 2x10^{-4}h \\ \left(\frac{\Delta}{a_g}\right)_{EC} = 0.02 \end{array}\right.$	$\frac{\Delta}{a_g} = 0.080 = 4\left(\frac{\Delta}{a_g}\right)_{EC}$
	$h \leq 380$ m	$h > 380$ m
B	$\frac{\Delta}{a_g} = max\left\{\begin{array}{l} 3.25x10^{-4}h \\ \left(\frac{\Delta}{a_g}\right)_{EC} = 0.030 \end{array}\right.$	$\frac{\Delta}{g} = 0.12 = 3.8\left(\frac{\Delta}{a_g}\right)_{EC}$
	$h \leq 400$ m	$h > 400$ m
C	$\frac{\Delta}{a_g} = \max\left\{\begin{array}{l} 3.25x10^{-4}h \\ \left(\frac{\Delta}{a_g}\right)_{EC} = 0.0345 \end{array}\right.$	$\frac{\Delta}{a_g} = 0.13 = 3.77\left(\frac{\Delta}{a_g}\right)_{EC}$
D	$\frac{\Delta}{a_g} = \max\left\{\begin{array}{l} 7x10^{-4}h \\ \left(\frac{\Delta}{a_g}\right)_{EC} = 0.054 \end{array}\right.$	

Using expression Eq (16) together with the value of Δ_0 given in Table 3, the $a_g(h)$ curves are given by solid lines in Fig. 18 to Fig. 21 for soil types A, B, C, and D, respectively. These curves can be used (based on the peak acceleration, soil depth, and soil type) to provide a means for the designer to evaluate whether a linear analysis is suitable for the given circumstances or not. It should be noted that comparing Fig. 16 and Fig. 18 it can be observed that using the expression of the EC for Δ_0 Eq (13) may result in an unacceptably poor approximation.

7 Numerical example

In the numerical example, soil type B was considered with shear wave velocity v = 600 m/s. We investigate one real and one artificial record. First, the record of the Northridge earthquake (Pacoima Dam station) was

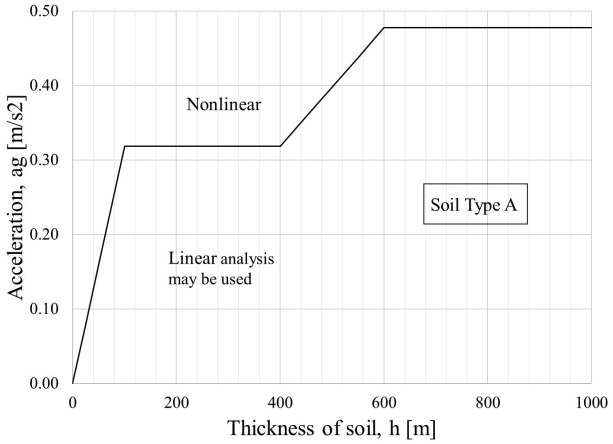

Fig. 18 Linear domain – enhanced Δ (below the solid line), Soil type A (v = 800 m/s), according to Eqs. (11), (13), (17) and Table 3

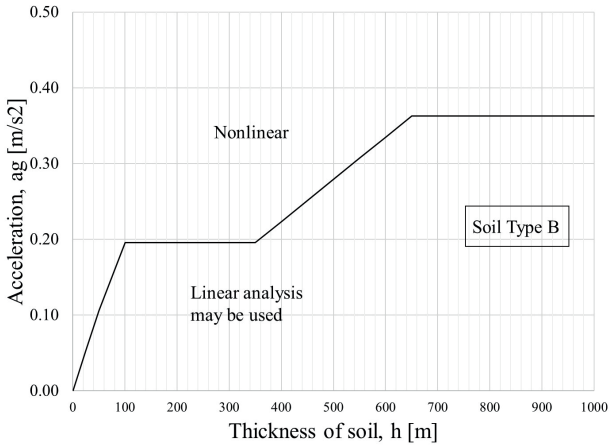

Fig. 19 Linear domain – enhanced Δ (below the solid line), Soil type B (v = 600 m/s), according to Eqs. (11), (13), (17) and Table 3

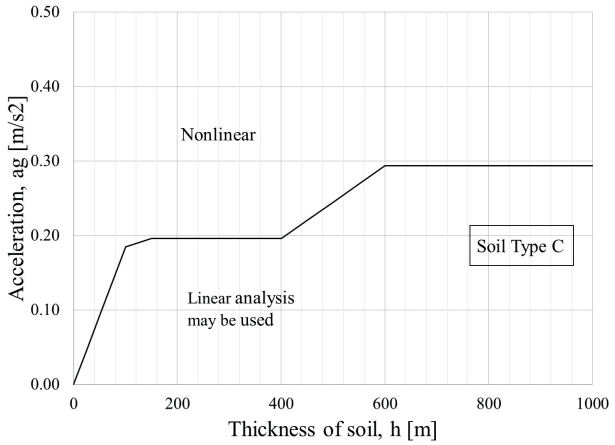

Fig. 20 Linear domain – enhanced Δ (below the solid line), Soil type C (v = 250 m/s), according to Eqs. (11), (13), (17) and Table 3

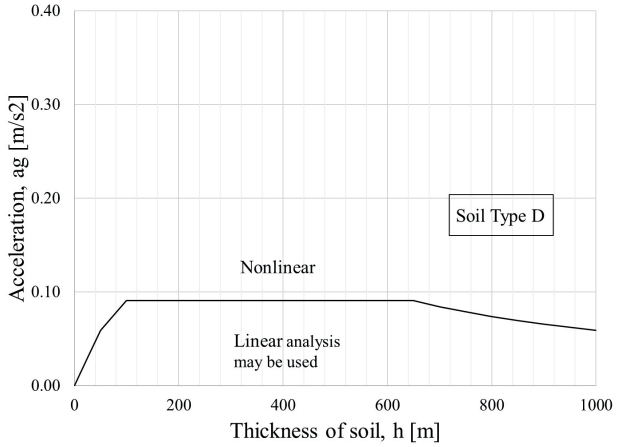

Fig. 21 Linear domain – enhanced Δ (below the solid line), Soil type D (v = 100 m/s), according to Eqs. (11), (13), (17) and Table 3

applied; the accelerogram is shown in Fig. 22. The maximum shear strain and the corresponding displacements were calculated as a function of the soil depth.

The results are shown in Fig. 23 and compared to our approximate formula. As can be seen, the approximation is quite accurate for $h \le h_L$ and conservative for higher values.

Next, one of the artificial records shown in Appendix A (Fig. 27) was applied to an h = 100 m thick soil layer. First, a linear analysis was performed. The $\gamma_L = 10^{-4}$ limit recorded at a_g = 0.196 m/s^2, while according to our model, it is recorded only at a_g = 0.195 m/s^2 as shown in Fig. 24.

The model results almost match the finite element results, as shown in Table 4.

As previously stated, soil stress-strain relationships are not always linear. Nonlinear analysis was performed to determine how the soil strain would be affected (Fig. 25). The soil parameters considered in the analysis were taken from EC8 recommendations, c = 70 kPa (soil cohesion)

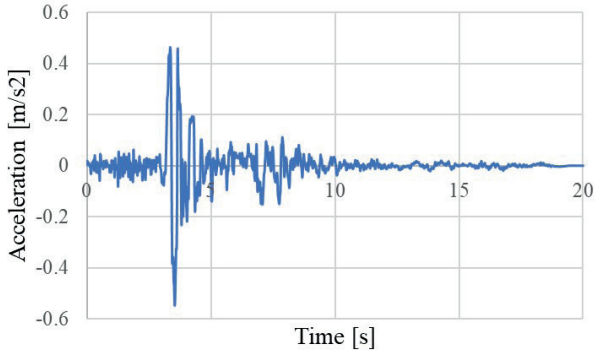

Fig. 22 Acceleration-time history of the seismic input

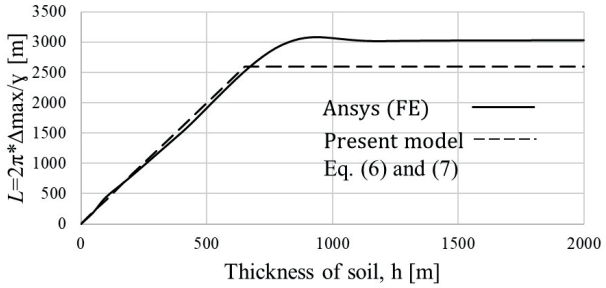

Fig. 23 Soil depth versus replacement wavelength for Northridge earthquake (1994)

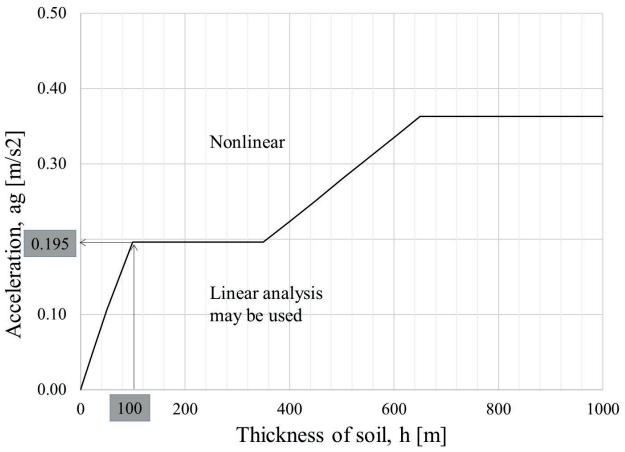

Fig. 24 Determination of the critical acceleration based on our model

and φ = 0 (friction angle). The Classic Drucker-Prager model has been used in this simulation. This model uses the outer cone approximation to the Mohr-Coulomb rule, which is applicable to these materials such as soils, rock, and concrete [25, 29]. The γ_L (calculated by Ansys) based on the above c and φ is $\gamma_L = 1.06 \times 10^{-4}$. The results of the nonlinear analysis comparing to the linear analysis and our model are shown in Fig. 26.

The limit value under which liner analysis may be used is obtained from Fig. 24; it is 0.195 m/s^2. It is given in Fig. 26 by dashed line. It shows quite accurately the limit of the linear analysis.

Table 4 Numerical examples results - linear and nonlinear analysis

ID	ag [g]	FE (Linear)		FE (Nonlinear)		Present model		$\frac{\Delta_{FE(linear)}}{\Delta_{EC}}$	$\frac{\gamma_{FE(linear)}}{\gamma_{Model}}$	$\frac{\gamma_{FE(nonlinear)}}{\gamma_{FE(linear)}}$
		Δ_{max} [m]	$\gamma_{FE(linear)}$	Δ_{max} [m]	$\gamma_{FE(nonlinear)}$	Δ [m]	$\gamma = 2\pi\,\Delta/L$			
1	0.005	0.00167	2.7E-05	0.0017	2.7E-05	0.00164	2.6E-05	1.02	1.03	1.00
2	0.01	0.00335	5.3E-05	0.0034	5.3E-05	0.00328	5.2E-05	1.02	1.03	1.00
3	0.02	0.0070	1.01E-04	0.0067	1.01E-04	0.00660	1.04E-04	1.05	0.98	1.00
4	0.04	0.0139	2.2E-04	0.0584	2.03E-03	0.0132	2.1E-04	1.06	1.06	9.27
5	0.10	0.0320	5.1E-04	0.830	3.45E-03	0.0329	5.1E-04	0.98	0.98	6.75

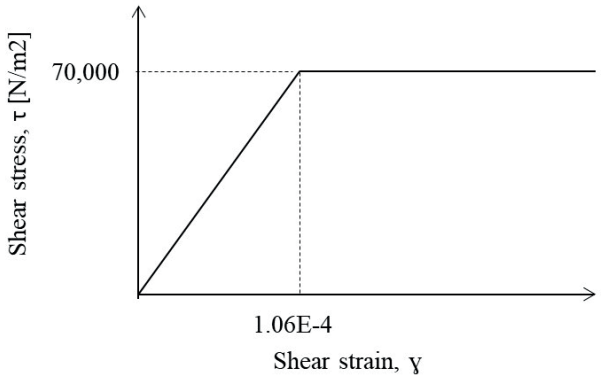

Fig. 25 Shear stress and strain relation used in the nonlinear analysis

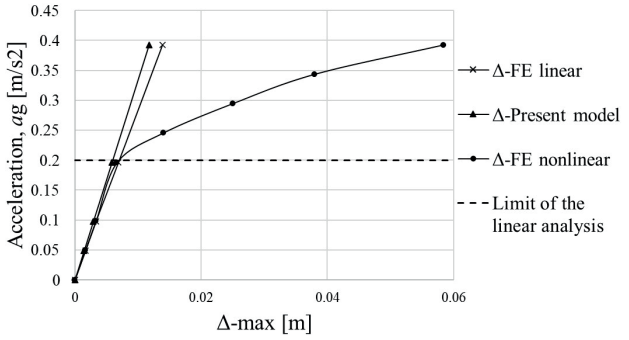

Fig. 26 Acceleration displacement curve for linear FE, nonlinear FE, and the present model

8 Conclusions

A simple model was developed to calculate the maximum shear strain (γ) in the soil subjected to earthquake excitation. It was found that can be calculated from PGA (a_g) and the maximum horizontal displacement of the ground (Δ):

$$\gamma = -\frac{2\pi}{L}\Delta,\ L = \min\begin{cases} 4h \\ 4\times 650m \end{cases},$$

where h is the thickness of the soil layer. This model – which is based on a 1D shear column – enables the designer to decide whether nonlinearity plays a role or not.

EC8 gives a recommendation for calculating Δ, which is independent of the thickness of the soil. It was found that this expression is conservative for shallow layers while underestimate Δ for thick layers. In this paper, a simple expression was suggested for the estimation of Δ which is the envelope of several time history analyses. Using these expressions, simple curves (Fig. 18 to Fig. 21) were determined as a function of a_g, soil depth, and soil type, which enables the designer to decide whether linear analysis may be performed. These graphs demonstrate that for soil types A, B, C, and D, the threshold acceleration of nonlinear soil behavior is around 0.48, 0.36, 0.29, and 0.10 m/s^2, respectively, depending on the depth of the soil. It is clearly shown that under moderate seismicity for shallow soil layers nonlinear analysis must be performed.

Finally, it's essential to acknowledge the strong sides of the proposed issue. A simple model with a few parameters can help researchers or designers estimate the soil's nonlinearity. However, it's also essential to consider the proposed issue's weak sides or limitations. Our hypothesis is verified under different excitations using a limited number of earthquake records. Conservative envelopes have been obtained. In addition, it has been verified for one layer of soil; therefore, it needs to be verified with two or more soil layers.

Acknowledgment

I would like to express my thanks to dr. Zsuzsa Borbála Pap for her support in Ansys modeling. My grateful thanks are also extended to the Stipendium Hungaricum scholarship, founded by the Hungarian Government, and managed by the Tempus Public Foundation.

References

[1] Kramer, S. "Geotechnical Earthquake Engineering", Pearson Education India, 1996. ISBN: 978-0133749434

[2] Wilson, E. L. "Three-dimensional static and dynamic analysis of structures", Computers and Structures Inc., 1996. ISBN: 0-923907-00-9

[3] Wolf, J. P. "Dynamic Soil-Structure interaction", Prentice Hall, 1985. ISBN: 978-0132215657

[4] Lai, C. G., Martinelli, M. "Soil-Structure Interaction Under Earthquake Loading: Theoretical Framework", ALERT Doctoral School 2013, Soil-Structure Interaction, The Alliance of Laboratories in Europe for Research and Technology, 2013, pp. 3–44, 2013.

[5] Ishihara, K. "Soil behaviour in earthquake geotechnics", [pdf] Clarendon Press, 1997. ISBN 0-19-856224-1 Available at: http://www4.hcmut.edu.vn/~cnan/DONG%20DAT%20Ishihara.PDF

[6] Kamgar, R., Gholami, F., Zarif Sanayei, H. R., Heidarzadeh, H. "Modified Tuned Liquid Dampers for Seismic Protection of Buildings Considering Soil–Structure Interaction Effects", Iranian Journal of Science and Technology, Transactions of Civil Engineering, 44(1), pp. 339–354, 2020. https://doi.org/10.1007/s40996-019-00302-x

[7] Tavakoli, R., Kamgar, R., Rahgozar, R. "Optimal Location of Energy Dissipation Outrigger in High-rise Building Considering Nonlinear Soil-structure Interaction Effects", Periodica Polytechnica Civil Engineering, 64(3), pp. 887–903, 2020. https://doi.org/10.3311/ppci.14673

[8] Tavakoli, R., Kamgar, R., Rahgozar, R. "Seismic performance of outrigger–belt truss system considering soil–structure interaction", International Journal of Advanced Structural Engineering, 11(1), pp. 45–54, 2019. https://doi.org/10.1007/s40091-019-0215-7

[9] Kamgar, R., Tavakoli, R., Rahgozar, P., Jankowski, R. "Application of discrete wavelet transform in seismic nonlinear analysis of soil–structure interaction problems", Earthquake Spectra, 37(3), pp. 1980–2012, 2021. https://doi.org/10.1177/8755293020988027

[10] Vucetic, M. "Cyclic Threshold Shear Strains in Soils", Journal of Geotechnical Engineering, 120(12), pp. 2208–2228, 1994. https://doi.org/10.1061/(ASCE)0733-9410(1994)120:12(2208)

[11] Hardin, B. O., Drnevich, V. P. "Shear Modulus and Damping in Soils: Measurement and Parameter Effects (Terzaghi Leture)", Journal of the Soil Mechanics and Foundations Division, 98(6), pp. 603–624, 1972. https://doi.org/10.1061/jsfeaq.0001756

[12] Atkinson, J. H. "Non-linear soil stiffness in routine design", Géotechnique, 50(5), pp. 487–508, 2000. https://doi.org/10.1680/geot.2000.50.5.487

[13] Atkinson, J. H. "Experimental determination of stress-strain-time characteristics in laboratory and-in-situ tests", In: Proceedings of the 10th European Conference on Soil Mechanics and Foundation Engineering (ECSMFE), 3, 1991, pp. 915–956. ISBN: 978-9054100041

[14] Drnevich, V. P., Richart Jr., F. E. "Dynamic Prestraining of Dry Sand", Journal of the Soil Mechanics and Foundations Division, 96(2), pp. 453–469, 1970. https://doi.org/10.1061/jsfeaq.0001398

[15] Idriss, I. M. "Response of soft soil sites during earthquakes", In: Proceedings of the Memorial Symposium to Honor Professor Harry Bolton Seed, Berkeley, CA, USA, II, 1990, pp. 273–289. ISBN: 9780921095101

[16] Chin, B.-H., Aki, K. "Simultaneous study of the source, path, and site effects on strong ground motion during the 1989 Loma Prieta earthquake: a preliminary result on pervasive nonlinear site effects", Bulletin of the Seismological Society of America, 81(5), pp. 1859–1884, 1991.

[17] Wen, K.-L., Beresnev, I. A., Yeh, Y. T. "Nonlinear soil amplification inferred from downhole strong seismic motion data", Geophysical Research Letters, 21(24), pp. 2625–2628, 1994. https://doi.org/10.1029/94gl02407

[18] Wu, C., Peng, Z., Ben-Zion, Y. "Refined thresholds for non-linear ground motion and temporal changes of site response associated with medium-size earthquakes", Geophysical Journal International, 182(3), pp. 1567–1576, 2010. https://doi.org/10.1111/j.1365-246x.2010.04704.x

[19] Rubinstein, J. L. "Nonlinear site response in medium magnitude earthquakes near Parkfield, California", Bulletin of the Seismological Society of America, 101(1), pp. 275–286, 2011. https://doi.org/10.1785/0120090396

[20] Ghofrani, H., Atkinson, G. M., Goda, K. "Implications of the 2011 M9.0 Tohoku Japan earthquake for the treatment of site effects in large earthquakes", Bulletin of Earthquake Engineering, 11(1), pp. 171–203, 2013. https://doi.org/10.1007/s10518-012-9413-4

[21] Wang, H.-Y., Jiang, W.-P., Wang, S.-Y., Miao, Y. "Correction to: In situ assessment of soil dynamic parameters for characterizing nonlinear seismic site response using KiK-net vertical array data", Bulletin of Earthquake Engineering, 17(5), 2361, 2019. https://doi.org/10.1007/s10518-018-00545-5

[22] "EN 1998-1:2004 Eurocode 8: Design of Structures for Earthquake Resistance - Part 1 General rules, seismic actions and rules for buildings", European Committee for Standardization, 2003.

[23] Pap, Z. B., Kollár, L. P. "Model of Soil-structure Interaction of Objects Resting on Finite Depth Soil Layers for Seismic Design", Periodica Polytechnica Civil Engineering, 63(4), pp. 1204–1216, 2019. https://doi.org/10.3311/ppci.14459

[24] "EN 1998-5:2004 Eurocode 8: Design of structures for earthquake resistance Part 5: Foundations, retaining structures and geotechnical aspects", European Committee for Standardization, 2003.

[25] ANSYS "ANSYS Mechanical APDL Material Reference", [online] Available at: https://www.scribd.com/document/259226150/ANSYS-Mechanical-APDL-Material-Reference

[26] Kuhlemeyer, R. L., Lysmer, J. "Finite Element Method Accuracy for Wave Propagation Problems", Journal of the Soil Mechanics and Foundations Division, 99(5), pp. 421–427, 1973. https://doi.org/10.1061/jsfeaq.0001885

[27] Pap, Z. B., Kollár, L. P. "Effect of Resonance in Soil-Structure Interaction for Finite Soil Layers", Periodica Polytechnica Civil Engineering, 62(3), pp. 676–684, 2018. https://doi.org/10.3311/ppci.11960

[28] FEMA "Quantification of Building Seismic Performance Factors", Washington, DC, USA, ATC-63 Project Report, 2009.

[29] Drucker, D. C., Prager, W. "Soil mechanics and plastic analysis or limit design", Quarterly of Applied Mathematics, 10(2), pp. 157–165, 1952. https://doi.org/10.1090/qam/48291

Appendix A

Response spectra corresponding to the artificial records.

The response spectra corresponding to the artificial records for soil types B, C and D are shown in Fig. 27 to Fig. 29, respectively.

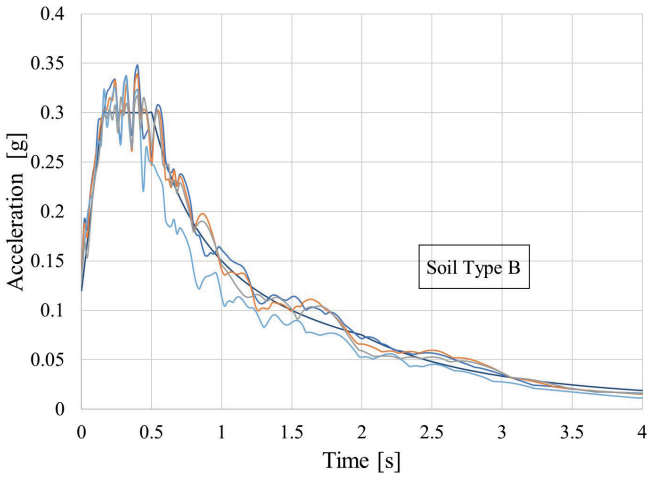

Fig. 27 Response spectra of artificial earthquake records generated for the given response spectrum to EC8 (a); Type B

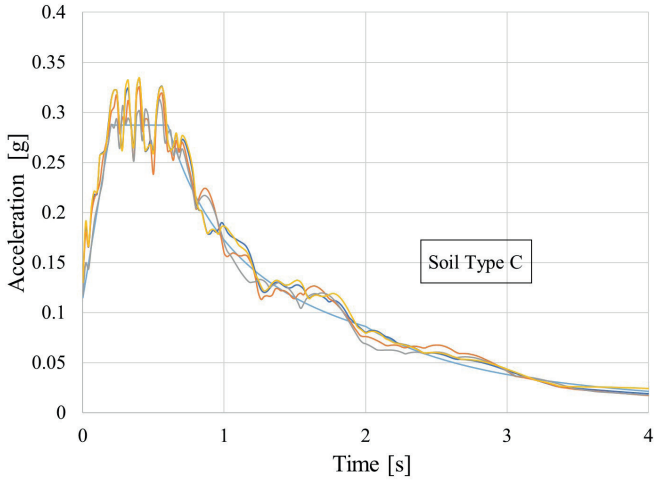

Fig. 28 Response spectra of artificial earthquake records generated for the given response spectrum to EC8 (a); Type C

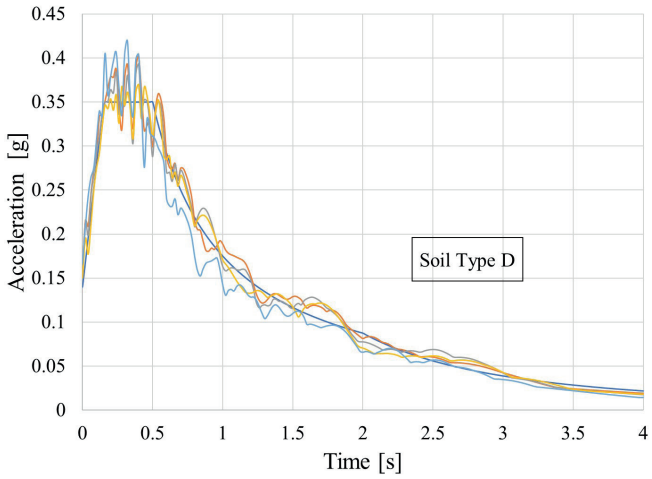

Fig. 29 Response spectra of artificial earthquake records generated for the given response spectrum to EC8 (a); Type D